

University of Groningen

Passivity-based harmonic control through series/parallel damping of an H-bridge rectifier

De Vries, M. M. J.; Kransse, M. J.; Liserre, M.; Monopoli, V. G.; Scherpen, J. M. A.

Published in:
Proceedings of the IEEE International Symposium on Industrial Electronics

IMPORTANT NOTE: You are advised to consult the publisher's version (publisher's PDF) if you wish to cite from it. Please check the document version below.

Document Version
Publisher's PDF, also known as Version of record

Publication date:
2007

[Link to publication in University of Groningen/UMCG research database](#)

Citation for published version (APA):

De Vries, M. M. J., Kransse, M. J., Liserre, M., Monopoli, V. G., & Scherpen, J. M. A. (2007). Passivity-based harmonic control through series/parallel damping of an H-bridge rectifier. In *Proceedings of the IEEE International Symposium on Industrial Electronics* (pp. 3385-3390). University of Groningen, Research Institute of Technology and Management.

Copyright

Other than for strictly personal use, it is not permitted to download or to forward/distribute the text or part of it without the consent of the author(s) and/or copyright holder(s), unless the work is under an open content license (like Creative Commons).

The publication may also be distributed here under the terms of Article 25fa of the Dutch Copyright Act, indicated by the "Taverne" license. More information can be found on the University of Groningen website: <https://www.rug.nl/library/open-access/self-archiving-pure/taverne-amendment>.

Take-down policy

If you believe that this document breaches copyright please contact us providing details, and we will remove access to the work immediately and investigate your claim.

Downloaded from the University of Groningen/UMCG research database (Pure): <http://www.rug.nl/research/portal>. For technical reasons the number of authors shown on this cover page is limited to 10 maximum.

Passivity-Based Harmonic Control through Series/Parallel Damping of an H-Bridge Rectifier

Martijn M.J. de Vries, Marco J. Kransse,

Delft Center for Systems and Control

Delft, The Netherlands (NL)

Email: {mmjdevries}{mjkranse}@hotmail.com

Marco Liserre, Vito G. Monopoli

Politecnico di Bari

Bary, Italy

Email: liserre@gmail.com

Jacquelin M.A. Scherpen

Fac. Math. & Natural Sc.

Groningen, NL. *Corr. author

Email: j.m.a.scherpen@rug.nl

Abstract—Nowadays the H-bridge is one of the preferred solutions to connect DC loads or distributed sources to the single-phase grid. The control aims are: sinusoidal grid current with unity power factor and optimal DC voltage regulation capability. These objectives should be satisfied, regardless the conditions of the grid, the DC load/source and the converter nonlinearities. In this paper a passivity-based approach is thoroughly investigated proposing a damping-based solution for the error dynamics. Practical experiments with a real converter validate the analysis.

I. INTRODUCTION

The single-phase Voltage Source Converter (VSC), also called H-bridge or full bridge, can be used as universal converter due to the possibility to perform DC/DC, DC/AC or AC/DC conversion [1]. Moreover, it can be used as basic cell of the cascade multilevel converters [2] and [3]. The control of this kind of converter has been subject of many scientific studies, though conventional lead-lag control techniques are most often applied in practice. However, recently the passivity-based approach [4] has been investigated both for single-phase and multilevel configurations [5]–[9]. One advantage of passivity-based control is the explicit use of knowledge of the physical system structure in the controller. For nonlinear systems this results in a nonlinear controller which is different from conventional controllers such as lead-lag. These nonlinear model based control methods can ensure better robust performance in presence of large set point changes and disturbances, since the full nonlinear dynamics are taken into account. In [9] a passivity control design method for output voltage regulation based on the Brayton-Moser framework, [10], is developed for DC-DC converters such that the closed loop system is robust against load variations. This method has been extended to the three-phase AC-DC Boost rectifier in [11]. A pre-compensation scheme in order to use the DC-DC scheme of [9] yields an AC-DC Boost closed-loop system where the output voltage is robust against load variation. In this paper, the single-phase VSC as AC-DC rectifier is studied, and similar passivity based control schemes are designed in order to deal with load variations. However, due to the specific single-phase structure, the designs of [11] are not straightforwardly extended. Therefore, an adaptation scheme is included in the designs, and robustness of these designs is tested in an experimental set-up.

Furthermore, the problem of grid current harmonic rejection has only been addressed for a limited class of converters, using the passivity-based theory, [12], [13]. For the single-phase

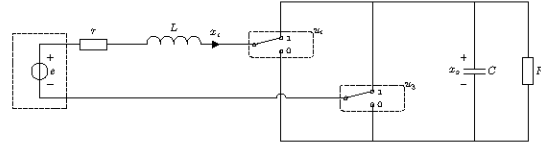


Fig. 1. Single-phase AC-DC boost converter with two ideal switches

grid connected application it is of particular interest, since the desired current is a sinusoidal quantity and its tracking is rather demanding [14]. This desired sinusoidal current is not corresponding to a constant output voltage and results in an output voltage with a ripple of 100 Hz [15]. In this paper, a dynamic damping injection scheme for the compensation of harmonic distortion is proposed. It is implemented by means of bandpass filters, with physical interpretation, that filter out higher harmonic distortion. The resulting design is experimentally validated on an H-bridge rectifier.

II. CONVERTER MODEL IN BRAYTON-MOSER FORM

A. Converter Dynamics

A single-phase AC-DC boost converter is shown in Fig. 1, where a parasitic input resistor with resistance r is in series with the input inductor to model dissipation effects in the converter. The inductance and capacitance are denoted by L and C respectively. The current through the inductor is denoted by x_1 and the voltage across the capacitor is denoted by x_2 . The converter is connected to an ideal sinusoidal voltage source $e = E \sin(\omega t)$. The load is assumed to be purely resistive and, moreover, the value of $G = R^{-1}$ is assumed to be constant but unknown. The digital switch inputs u_1 and u_3 of the converter are controlled with pulse width modulation and corresponding duty ratios μ_1 and μ_3 . If pulse width modulation is applied and the switching frequency is sufficiently high, then an averaged mixed-potential function can be derived [4], [9], [15].

In [9] passivity-based controllers are tuned with help of modified stability theorems originally proposed by Brayton and Moser [10]. The presented tuning method is based on the averaged mixed-potential function. If the vector z is defined as $z = [z_1 \ z_2]^T$, then in case of the single-phase AC-DC boost converter it can be shown that the averaged mixed-potential function can be decomposed as

$$P(e, z, \mu) = P_T(\mu, z) + P_D(z) + P_F(e, z) \quad (1)$$

with the individual terms of the form

$$P_T(\mu, z) = \mu z_1 z_2 \quad (2)$$

$$P_D(z) = P_R(z) - P_G(z) = \frac{1}{2} r z_1^2 - \frac{1}{2} G z_2^2 \quad (3)$$

$$P_F(e, z) = -e z_1 \quad (4)$$

with the average inductor current z_1 and the average capacitor voltage z_2 . The continuous function μ is defined as $\mu = \mu_1 - \mu_3$, with $\mu_1 \in [0, 1]$ and $\mu_3 \in [0, 1]$. By definition of the averaged mixed-potential function it holds true that

$$Q\dot{z} = \nabla_z P(e, z, \mu), \quad Q = \begin{bmatrix} -L & 0 \\ 0 & C \end{bmatrix} \quad (5)$$

where ∇_z denotes the n -dimensional gradient with respect to $z = [z_1, \dots, z_n]^T$. The term $P_T(\mu, z)$ represents the power circulating across the dynamic elements. The dissipative current-potential $P_R(z)$ and the dissipative voltage-potential $P_G(z)$ capture the influence of current-controlled and voltage-controlled resistors respectively. The total power that is absorbed by the source is denoted by $P_F(e, z)$. With help of (5) it can be verified that the dynamics of the average state model is described by the differential equations

$$-L\dot{z}_1 = \mu z_2 + r z_1 - e \quad (6)$$

$$C\dot{z}_2 = \mu z_1 - G z_2 \quad (7)$$

B. Control Objectives

The control objectives are formulated as

- The output voltage has to be equal to V_d .
- The input current has to be sinusoidal and in phase with the input voltage.

The direct control of the output voltage leads to an internally unstable controller due to the unstable zero-dynamics with respect to the average output voltage [15], [16]. Therefore a passivity-based controller has to be designed such that it indirectly controls the output voltage by controlling the input current. To achieve zero total harmonic current distortion and unity power factor the desired sinusoidal input current z_1^* is chosen in phase with the input voltage, i.e.,

$$z_1^* = I_d \sin(\omega t) \quad (8)$$

As a consequence of this sinusoidal input current, as demonstrated in [15] and [5], the output voltage will inevitable have a 100 Hz ripple. Because of this ripple the first control objective cannot be satisfied and therefore, the control objectives are reformulated as:

- The root mean square (RMS) value of the output voltage has to be equal to V_d .
- The input current has to be sinusoidal and in phase with the input voltage.

To obtain a desired RMS value V_d of the output voltage, from the power balance it can be concluded that I_d has to be of the form

$$I_d = \frac{E - \sqrt{E^2 - 8rGV_d^2}}{2r} \quad (9)$$

where, to obtain a real solution, it is required that

$$V_d \leq \sqrt{\frac{E^2}{8rG}} \quad (10)$$

C. Co-Energy Storage Function

The concept of energy is important in passivity-based control [4], [17]–[19]. The single-phase converter contains two storage elements and the co-energy storage function can be formulated as $H^*(z) = \frac{1}{2} L z_1^2 + \frac{1}{2} C z_2^2$. It describes the total co-energy in the two dynamic elements and can be shaped and used for closed-loop stability.

III. PASSIVITY-BASED CONTROLLER DESIGN

First a controller is designed for the converter with the load assumed to be known. Then the load is assumed to be unknown and the controller is extended with a load estimation.

A. Controller Design: Known Parameter Case

Generally speaking, the design procedure for a passivity-based controller consists of modifying the co-energy such that for the closed-loop system the minimum is in the desired equilibrium of the closed-loop system. In addition to this step, the dissipation structure is modified to damp the errors in the state variables [4], [9]. If the average state error vector is defined as $\tilde{z} = z - \xi$, with ξ the controller state vector, and the desired closed-loop co-energy function is chosen as $H_d^*(\tilde{z}) = H^*(z)|_{z=\tilde{z}}$, then the controller design procedure can be summarized as follows.

The closed-loop error dynamics is determined by making a partial copy of the system in Brayton–Moser form and by replacing the state vector z with the state error vector \tilde{z} . As an essential part of the controller design procedure, the dissipation structure is modified by adding a damping injection term $P_V(\tilde{z})$ to the dissipation potential $P_D(z)|_{z=\tilde{z}}$, resulting in a modified dissipation potential $P_M(\tilde{z})$, i.e., $P_M(\tilde{z}) = P_D(z)|_{z=\tilde{z}} + P_V(\tilde{z})$. In Brayton–Moser form the desired closed-loop error dynamics is described by

$$Q\dot{\tilde{z}} = \nabla_{\tilde{z}} \left[P_T(\mu, z)|_{z=\tilde{z}} + P_M(\tilde{z}) \right] \quad (11)$$

where the matrix Q is assumed to be constant corresponding to the linear dynamic elements i.e., Q is as in (5). If the modified dissipation potential is quadratic in \tilde{z} , then the controller dynamics is implicitly described by

$$Q\dot{\xi} = \nabla_{\xi} P_c(e, z, \mu, \xi) \quad (12)$$

$$P_c(e, z, \mu, \xi) = P_T(\mu, z)|_{z=\xi} + P_D(z)|_{z=\xi} + P_F(e, z)|_{z=\xi} - P_V(\tilde{z}) \quad (13)$$

To obtain an explicit controller description (12) is solved for μ with respect to the minimum phase state $\xi_1 = z_1^* = I_d \sin(\omega t)$. In case of the single-phase converter the controller dynamics is described by the two differential equations

$$\begin{aligned} \mu &= \frac{e - r z_1^* + r_i(z_1 - z_1^*) - L \dot{z}_1^*}{\xi_2} \\ C \dot{\xi}_2 &= \mu z_1^* - G \xi_2 + G_i(z_2 - \xi_2), \quad \xi_2(0) > 0 \end{aligned} \quad (14)$$

The term r_i is interpreted as the series damping injection term acting on the current error and G_i is interpreted as the parallel damping injection term acting on the voltage error. The damping injection is chosen with the tuning rules from [9]. These tuning rules are based on the theory of Brayton–Moser [10] and they provide a lower bound for the injected damping to ensure convergence of the closed-loop error state in a non-oscillatory way. Interestingly, to obtain non-oscillatory convergence only one type of damping is required and in case of the series damping injection strategy the lower bound for the damping is given as

$$r_i(\mu) = \frac{1}{1-\delta} \sqrt{\frac{\mu^2 L}{C}} - r \quad G_i(\mu) = 0 \quad (15)$$

with tuning parameter $\delta \in (0, 1)$. In case of the parallel damping injection the lower bound for the damping is given as

$$G_i(\mu) = \frac{1}{1-\delta} \sqrt{\frac{\mu^2 C}{L}} - G \quad r_i(\mu) = 0 \quad (16)$$

with tuning parameter $\delta \in (0, 1)$.

B. Controller Design: Unknown Parameter Case

In the previous part the value of the load G is assumed to be known, but in reality this assumption might be invalid. Therefore, as in [6] and [7], an estimator is used to estimate the correct value of G . The estimation error is defined as $\tilde{G} = \hat{G} - G$ where \hat{G} is the estimated value. By replacing G with \hat{G} , the controller is explicitly described by

$$\mu = \frac{e - rz_1^* + r_i(z_1 - z_1^*) - L\dot{z}_1^*}{\xi_2} \quad (17)$$

$$C\dot{\xi}_2 = \mu z_1^* - \hat{G}\xi_2 + G_i(z_2 - \xi_2) \quad (18)$$

The analysis of convergence goes along similar lines as in Section III.A. To make sure that the perturbation term $\tilde{G}\xi_2$ converges to zero the estimator is chosen as in [4], i.e.,

$$\dot{\hat{G}} = \dot{\tilde{G}} = -\alpha(z_2 - \xi_2)\xi_2 \quad (19)$$

where the adaption gain $\alpha > 0$ is a tuning parameter. The control dynamics is described by (17), (18) and (19) with the desired current amplitude of the form

$$I_d = \frac{E - \sqrt{E^2 - 8rV_d^2\hat{G}}}{2r} \quad (20)$$

and $z_1^* = I_d \sin(\omega t)$ and \dot{z}_1^* is

$$\dot{z}_1^* = \omega I_d \cos(\omega t) + \frac{dI_d}{d\hat{G}} \sin(\omega t) \dot{\hat{G}}$$

When the series damping injection strategy is applied, there are no changes in (15), but in case of the parallel damping injection strategy, the value for the load G has to be replaced with its estimate \hat{G} in (16), resulting in

$$G_i(\mu) = \frac{1}{1-\delta} \sqrt{\frac{\mu^2 C}{L}} - \hat{G} \quad R_i(\mu) = 0 \quad (21)$$

Practical results with this adaptive controller are shown in Sect. V.

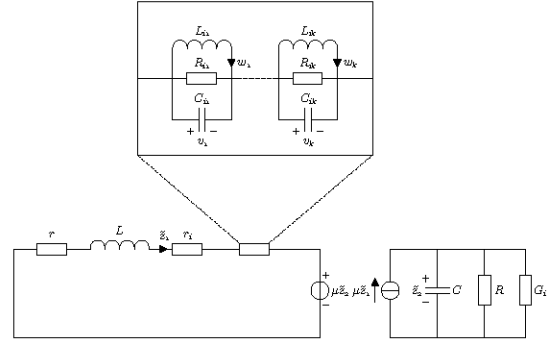


Fig. 2. Closed-loop network interpretation for the passivity-based controlled power converter with k bandpass filters

IV. CURRENT SHAPE IMPROVEMENT

A. Problem Formulation

The input current of the single-phase AC–DC boost converter contains harmonics due to internal causes (non-ideal transistors and diodes, blanking times and saturation in the grid-side inductor) and external causes (grid harmonics). Evidently, to obtain a lower total harmonic current distortion and a higher power factor the current shape has to be improved. Without redesigning the converter and inspired by the preliminary results in [13], a passivity-based controller that is based on the frequency domain description of periodic disturbances can accomplish this.

B. Controller Design: Known Parameter Case

Suppose that to meet the design specifications k current harmonics have to be reduced in amplitude. For reasons of simplicity, it is initially assumed that the value of G is known. To add the damping injection filters to the closed-loop system, for each individual frequency to be compensated for a virtual parallel RLC network is included (see Sect. IV-D). The desired closed-loop representation is shown in Fig. 2 and in accordance with this representation the desired closed-loop error equations are formulated as

$$L\dot{\tilde{z}}_1 = -(r + r_i)\tilde{z}_1 - \sum_{h=1}^k v_h - \mu\tilde{z}_2 \quad (22)$$

$$C\dot{\tilde{z}}_2 = \mu\tilde{z}_1 - (G + G_i)\tilde{z}_2 \quad (23)$$

$$L_{ih}\dot{w}_h = v_h \quad (24)$$

$$C_{ih}\dot{v}_h = \tilde{z}_1 - \frac{1}{R_{ih}}v_h - w_h \quad (25)$$

with $h \in \{1, \dots, k\}$. Notice that the closed-loop error equations are similar to the equations that describe the dynamics of the average state model (6)–(7). The latter two equations describe the dynamics of a bandpass filter. It can be proved by standard techniques that the equilibrium point $[\tilde{z}^T v^T w^T]^T = 0$ is asymptotically stable. To actually obtain the desired closed-loop error equations the passivity-based controller is explicitly

described by

$$\mu = \frac{e - L\dot{z}_1^* - rz_1^* + r_i(z_1 - z_1^*) + \sum_{h=1}^k v_h}{\xi_2} \quad (26)$$

$$C_{ih}\dot{v}_h = z_1 - z_1^* - \frac{1}{R_{ih}}v_h - w_h \quad (27)$$

$$L_{ih}\dot{w}_h = v_h \quad (28)$$

$$C\dot{\xi}_2 = \mu z_1^* - G\xi_2 + G_i(z_2 - \xi_2) \quad (29)$$

with I_d as described in (9), $z_1^* = I_d \sin(\omega t)$, $h \in \{1, \dots, k\}$ and $\xi_2(0) > 0$ assuming that the desired output voltage is positive.

C. Controller Design: Unknown Parameter Case

For this controller it holds true that the value of the load G is unknown and the previous controller is extended with an estimator. This extension is made in a similar way as in Sect. III-B. Again it is assumed that k current harmonics have to be reduced and the desired closed-loop error equations are formulated as in equation (22), (24), (25) and

$$C\dot{\tilde{z}}_2 = \mu\tilde{z}_1 - (G + G_i)\tilde{z}_2 + \tilde{G}\xi_2 \quad (30)$$

with $h \in \{1, \dots, k\}$. It can be observed that the closed-loop error equations are similar to the equations that describe the dynamics of the average state model (6)–(7), but compared to the known parameter case a perturbation term (i.e., $\tilde{G}\xi_2$) is present. The estimator dynamics is chosen as

$$\dot{\tilde{G}} = \dot{G} = -\alpha(z_2 - \xi_2)\xi_2 \quad (31)$$

with the adaption gain $\alpha > 0$. To actually obtain the desired closed-loop error equations the controller is explicitly described by (26)–(28), (31) and

$$C\dot{\xi}_2 = \mu z_1^* - \hat{G}\xi_2 + G_i(z_2 - \xi_2) \quad (32)$$

with I_d as described in (20), z_1^* as described in (21), $h \in \{1, \dots, k\}$, and $\xi_2(0) > 0$ to prevent division by zero.

D. Damping Injection Filter Design

It can be verified that the transfer function of each damping injection filter can be described by

$$T_{ih}(s) = \frac{V_{ih}(s)}{\tilde{Z}_1(s)} = \frac{\frac{1}{C_{ih}}s}{s^2 + \frac{1}{R_{ih}C_{ih}}s + \frac{1}{L_{ih}C_{ih}}} \quad (33)$$

The parameters L_{ih} , R_{ih} and C_{ih} are related to important properties such as bandwidth and resonance frequency (see Table I). In general, the values of these parameters are not known a priori. This means that the spectrum of the input current has to be examined and based on this spectrum it has to be decided which frequencies have to be compensated for. In other words, the eigenfrequencies of the filters are fixed. The bandwidth of each filter should be chosen small but large enough to allow deviations in the input frequency. However, the gains of the filters should be chosen reasonably large to suppress the frequencies to be compensated for. This damping injection filter design approach is followed in Sect. V.

TABLE I

DESIGN PARAMETERS FOR THE DAMPING INJECTION FILTERS

Parameter			
Eigenfrequency of the filter	ω_0	$= \sqrt{\frac{1}{L_{ih}C_{ih}}}$	[rad/s]
Bandwidth (cut off at -3dB)	B	$= \frac{1}{R_{ih}C_{ih}}$	[rad/s]
Filter gain at ω_0	K	$= \frac{1}{R_{ih}}$	[V/A]

V. EXPERIMENTAL RESULTS

The design procedure reported in the paper is validated using a laboratory prototype in the Power Electronics Laboratory of DEE, Polytechnic of Bari. The converter that is used for the experiments is the Danfoss VLT 5006. This is a commercial three-phase rectifier/inverter combination, but in this case the converter is modified and it is used as a single-phase boost converter by using only two switching legs of the inverter. In each leg the switches are implemented by means of two Insulated Gate Bipolar Transistors (IGBT). The original Interface and Protection Card (IPC) is replaced with an IPC developed by the Aalborg University to provide external control over the gate signals. This IPC is optically driven by a dSPACE DS1104 board. For each leg only one control signal is needed, because the complementary control signal of the second IGBT is generated by the IPC itself. A dead-time of 2 μ s is taken into account.

The input current and output voltage are measured and both signals are filtered by a low pass RC filter with a cut-off frequency of 2 kHz (to remove the ripple introduced by the PWM). The filtered signals are fed back into the controller. The controller generates a PWM signal that is sent to the IPC through the optical link.

The parameters of the system are given in Table II.

TABLE II

PARAMETERS OF THE SINGLE-PHASE AC–DC BOOST CONVERTER FOR EXPERIMENTS

Parameter			
Input voltage amplitude	E	$= 100$	[V]
Input voltage frequency	$\omega/2\pi$	$= 50$	[Hz]
Capacitance	C	$= 340$	[μ F]
Inductance	L	$= 10$	[mH]
Parasitic resistance	r	≈ 2.5	[Ω]
PWM frequency	f_s	$= 12.8$	[kHz]
Desired output voltage	V_d	$= 200$	[V]
Initial load	G	$= \frac{1}{220}$	[Ω^{-1}]

The power dissipation in the converter is modeled by means of a parasitic resistor with resistance r . Since this value cannot be measured it is chosen in such a way that the RMS value of the output voltage is as desired and the input current is (close to) the desired current (i.e., RMS value and phase of the input current are as desired). For this initial set-up the value is chosen to be equal to $r = 2.5 \Omega$.

A. Robustness to Load Variation

The controller as described in Sect. III-B is connected to the converter. Justified by the tuning rules only one type of

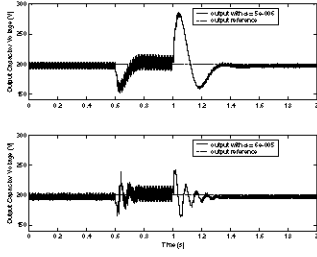


Fig. 3. Output voltage z_2 for the series damping injection scheme during the step-wise load variation, using a low (top) and high (bottom) adaption gain.

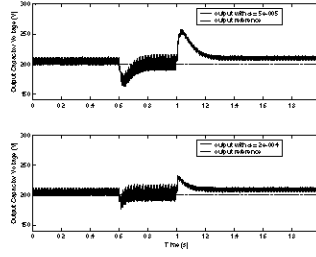


Fig. 4. Output voltage z_2 for the parallel damping injection scheme during the step-wise load variation, using a low (top) and high (bottom) adaption gain.

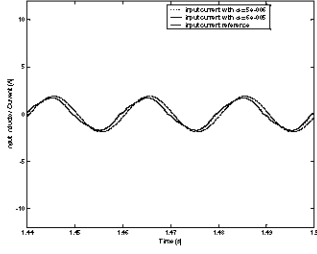


Fig. 5. Input current z_1 for the series damping injection scheme with $G = \frac{1}{440} \Omega^{-1}$, zoomed in at steady state, using a low (dotted) and high (solid) adaption gain.

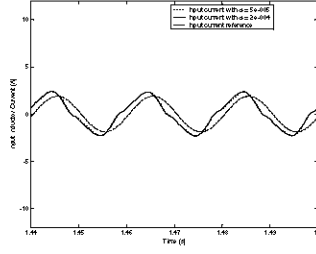


Fig. 6. Input current z_1 for the parallel damping injection scheme with $G = \frac{1}{440} \Omega^{-1}$, zoomed in at steady state, using a low (dotted) and high (solid) adaption gain.

damping injection is used at the same time i.e., either (15) or (21). Two different adaption gains are used and the adaption gains are chosen by observing the converter output. The high adaption gain in the experiments is approximately 80% of the adaption gain that causes the system to behave in an undesired way e.g., causing undesired oscillatory behavior or an over-current through the switches. The low adaption gain is chosen by evaluating the response of the system. In practice, this approach results in different adaption gain values for the series and parallel damping injection schemes. The load is varied step-wise in the following way

$$G = \frac{1}{R} = \begin{cases} \frac{1}{220} \Omega^{-1} & \text{for } 0 < t \leq 0.6 \\ \frac{1}{110} \Omega^{-1} & \text{for } 0.6 < t \leq 1 \\ \frac{1}{440} \Omega^{-1} & \text{for } 1 < t \leq 2 \end{cases}$$

1) *Series Damping Injection*: For this strategy, the damping injection is described by (15). In theory the steady state behavior does not depend on the value of the tuning parameter δ . Therefore, often the value $\delta = 0.5$ is chosen. In practice however, for low values of δ the input current is not sinusoidal and therefore the tuning parameter value is increased to $\delta = 0.9$. The output voltage z_2 and the input current z_1 during the load changes are shown in Fig. 3 and Fig. 5 respectively. In the results the 100 Hz ripple in the output voltage is clearly visible. The amplitude of this ripple depends on the system parameters and, as a consequence, on the load as well. During the variation in the load the RMS value of the output voltage returns to the desired output voltage within a boundary of

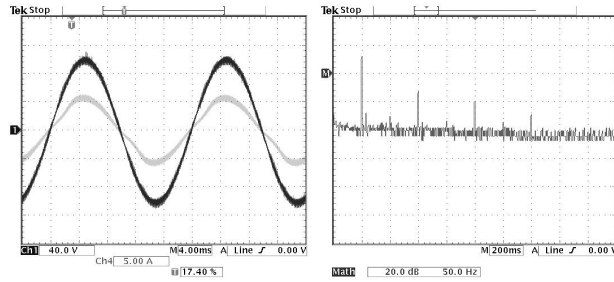
2%. From (19) it is clear that the load estimator dynamics depends on the error in the output voltage \tilde{z}_2 . Since this error is not damped the output of the estimator (not shown here for reasons of space) shows an oscillatory response. When the adaption gain is increased the frequencies of these oscillations are increased, as well as the frequencies of the oscillations in the output voltage. However, the maximum output voltage error decreases. A look at the currents reveals that they are in phase with the current reference. However, the currents are not purely sinusoidal which is caused by model mismatch (nonlinear plant characteristics and grid harmonics). For example, the nonlinear characteristics of the diodes and transistors are unmodeled. This also causes the RMS value of the output voltage and the output of the load estimator not to converge to their desired values. In steady state the maximum error of the load estimator in the experiment is approximately 20 Ω .

2) *Parallel Damping Injection*: For this strategy the damping injection is described by (21). Increasing the value of the tuning parameter δ does not significantly influence the current waveform. Therefore, the tuning parameter value is $\delta = 0.5$. The output voltage z_2 and the input current z_1 during the load changes are shown in Fig. 4 and Fig. 6 respectively. In contrast to the series damping injection scheme the overshoot in the output voltage during load variations is less. Moreover, after a load change with parallel damping injection oscillations in the load estimator output and the output voltage are absent. For all loads the RMS value of the output voltage is higher than the desired value, but it remains within a boundary of 5%. The input current is higher than the desired current, out of phase and more distorted. An explanation for this can be found in the fact that in case of series damping injection the input current is damped to a fixed desired input current z_1^* . In case of parallel damping injection the output voltage is damped to a desired output voltage trajectory ξ_2 . This is a dynamic state of the controller and therefore the parallel damping injection scheme is more sensitive to modeling errors. In steady state the maximum error of the load estimator in the experiment is approximately 80 Ω .

B. Current Shape Improvement

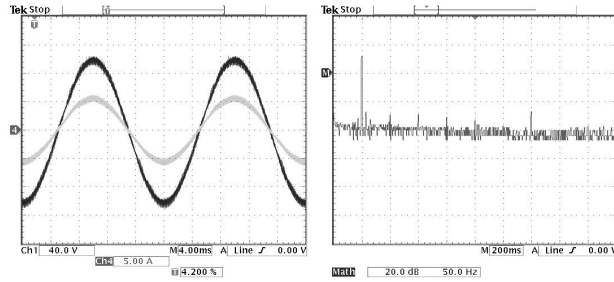
From the previous part it is clear that in case of series injected damping the input current waveform is more sinusoidal than in case of parallel injected damping. For further improvement of the input current waveform damping injection filters are added to the series damping injection scheme.

When no damping injection filters are used and the load is equal to $\frac{1}{170} \Omega^{-1}$, then the waveform and frequency spectrum of the input current are as shown in Fig. 7. From the frequency spectrum it can be seen that the harmonic content of the current is dominated by the third and fifth current harmonic. To lower the total harmonic current distortion and to improve the power factor these two harmonics are compensated for. The resonant frequencies of the two bandpass filters coincide with the frequencies of the two current harmonics (i.e., 150 Hz and 250 Hz). The bandwidth of each filter is chosen as 2 Hz to



(a) Input voltage e (black) and input current z_1 (grey) (b) Frequency spectrum of the input current z_1

Fig. 7. The input voltage e and input current z_1 with series damping injection and without filtering



(a) Input voltage e (black) and input current z_1 (grey) (b) Frequency spectrum of the input current z_1

Fig. 8. The input voltage e and input current z_1 with series damping injection and with filtering

allow small frequency deviations. These deviations are caused by the fact that in practice the fundamental frequency deviates from 50 Hz. Summarizing, the parameter values are shown in Table III.

TABLE III
PARAMETER VALUES OF THE TWO DAMPING INJECTION FILTERS

Parameter		Filter 3rd harmonic	Filter 5th harmonic	
Filter Gain	R_{ih}	= 400	300	[Ω]
Filter Inductance	L_{ih}	= 5.7	1.5	[mH]
Filter Capacitance	C_{ih}	= 198.94	265.26	[μ F]

When these damping injection filters are used, then the resulting current waveform and frequency spectrum are shown in Fig. 8. As desired, after comparison with the frequency spectrum in Fig. 7 it is clear that the third and fifth current harmonic are reduced. When the filters are added the current waveform is evidently more sinusoidal.

VI. CONCLUSION

In this paper a passivity-based controller is designed for a single-phase H-bridge rectifier. The control scheme with series damping injection is able to reduce the error in the input current in contrast to the control scheme with parallel damping injection. If the load estimator is added to the control scheme, then the estimated load and the output voltage with the series damping injection scheme contain more oscillations during

a step-wise load variation than with the parallel damping injection scheme. This is related to the fact that with parallel damping injection the output voltage error is damped. For the series damping injection scheme the addition of damping injection filters results in a reduction of selected current harmonics.

REFERENCES

- [1] B. K. Bose, *Modern Power Electronics and A.C. Drives*, 1st ed. Prentice Hall, 2001.
- [2] J. S. Lai and F. Z. Peng, "Multilevel converters – a new breed of power converters," *IEEE Transactions on Industrial Applications*, vol. 32, pp. 509–517, 1996.
- [3] C. Cecati, A. Dell'Aquila, M. Liserre, and V. G. Monopoli, "Design of h-bridge multilevel active rectifier for traction systems," *IEEE Transactions on Industry Applications*, vol. 39, pp. 1541–1550, 5 2003.
- [4] R. Ortega, A. Loria, P. J. Nicklasson, and H. Sira-Ramírez, *Passivity-based Control of Euler-Lagrange Systems*. Springer-Verlag, 1998.
- [5] D. Karagiannis, E. Mendes, A. Astolfi, and R. Ortega, "An experimental comparison of several pwm controllers for a single-phase ac-dc converter," *IEEE Transactions on Control Systems Technology*, vol. 11, no. 6, pp. 940–947, 2003.
- [6] G. Escobar, D. Chevreau, R. Ortega, and E. Mendes, "An adaptive Passivity-based controller for a unity power factor rectifier," *IEEE Transactions on Control Systems Technology*, vol. 9, no. 4, pp. 637–644, 2001.
- [7] C. Cecati, A. Dell'Aquila, M. Liserre, and V. G. Monopoli, "A Passivity-based multilevel active rectifier with adaptive compensation for traction applications," *IEEE Transactions on Industry Applications*, vol. 39, no. 5, pp. 1404–1413, 2003.
- [8] A. Dell'Aquila, M. Liserre, V. G. Monopoli, and P. Rotondo, "An energy-based control for an n-h-bridges multilevel active rectifier," *IEEE Transactions on Industrial Electronics*, vol. 52, no. 3, pp. 670–678, 2005.
- [9] D. Jeltsema and J. M. A. Scherpen, "Tuning of Passivity-preserving controllers for switched-mode power converters," *IEEE Transactions on Automatic Control*, vol. 49, no. 8, pp. 1333–1344, 2004.
- [10] R. K. Brayton and J. K. Moser, "A theory of nonlinear networks, part I," *Quart. Appl. Math.*, vol. 12, no. 1, pp. 1–33, 1964.
- [11] D. Jeltsema, J. M. A. Scherpen, and E. Hageman, "A robust passive power-based control strategy for three-phase voltage source rectifiers," *Proc. IFAC World Congress, Prague*, p. No. 4049, 2005.
- [12] G. E. Valderrama, P. Mattavelli, and A. M. Stanković, "Reactive power and imbalance compensation using STATCOM with dissipativity-based control," *IEEE Transactions on Control Systems Technology*, vol. 9, no. 5, pp. 718–727, 2001.
- [13] G. Escobar, A. M. Stanković, P. Mattavelli, and J. Leyva, "An adaptive control for UPS to compensate unbalance and harmonic distortion using a combined capacitor/load current approach," *Industrial Electronics Society, 2003. IECON 03. The 29th Annual Conference of the IEEE*, 2003.
- [14] R. Teodorescu, F. Blaabjerg, U. Bojrup, and M. Liserre, "A new control structure for grid-connected lcl pv inverters with zero steady-state error and selective harmonic compensation," *Proc. of APEC 2004*, vol. 1, pp. 580–586, 2004.
- [15] M. van Agthoven, "Tuning rules for the Passivity-based controller in the Brayton Moser setting, applied to the full-bridge AC–DC boost rectifier," Master's thesis, Delft University of Technology, 2003.
- [16] G. Escobar, "On nonlinear control of switching power electronics systems," Ph.D. dissertation, Laboratoire des signaux et systèmes, 1999.
- [17] A. J. van der Schaft, *\mathcal{L}_2 -Gain and Passivity techniques in nonlinear control*. Springer, 2000.
- [18] D. Jeltsema and J. M. A. Scherpen, "A dual relation between port-Hamiltonian systems and the Brayton-Moser equations for nonlinear switched RLC circuits," *Automatica*, vol. 39, pp. 969–979, 2003.
- [19] D. Jeltsema, "Modeling and control of nonlinear networks, a Power-based perspective," Ph.D. dissertation, Delft University of Technology, 2005.